ChemPubSoc Europe

DOI: 10.1002/ejic.201800831

EurJIC European Journal of Inorganic Chemistry

Full Paper

P–N Adducts | *Very Important Paper* |

2,2′-Azobispyridine in Phosphorus Coordination Chemistry: A New Approach to 1,2,4,3-Triazaphosphole Derivatives

Yulia S. Panova,[a] Alexandra V. Sheyanova,[a] Nataliya V. Zolotareva,[a] Vyacheslav V. Sushev,[a] Alla V. Arapova,[a] Alexander S. Novikov,[b] Evgenii V. Baranov,[a,c] Georgy K. Fukin,[a] and Alexander N. Kornev*[a]

Abstract: Oxidative addition of 2,2′-azobispyridine (*abpy*) to PCl_3 in CH_2Cl_2 or THF gave the 1:1 addition product, containing phosphorus in high oxidation state (+5) and a reduced form of the ligand. 2,2′-Hydrazobispyridine (*hbpy*) was prepared by reduction of *abpy* with hydrazine-hydrate in 63 % yield. Interaction of *hbpy* with PCl_3 in the presence of triethylamine gave $(abpy)^{2-}PCl$ (**2**) in 25 % preparative yield. A similar reaction of *hbby* with $(Et_2N)_2PCl$ afforded $(abpy)^{2-}PNEt_2$ (**4**) in 89 % yield. Compound **4** after work-up with PCl_3 or PBr_3 gave **2** and $(abpy)^{2-}PBr$ (**6**) respectively in high yields. Diethylamino-derivative **4** formed (κ^2-*N*,*N*) adduct with $SiCl_4$ **7** (coordination by Py and azo-functions), while the chloro-derivative **2** did not. Reaction of **2** with PCl_5 is accompanied with liberation of PCl_3 and formation of spirocyclic *ate* complex $[(abpy)^{2-}{}_2P]^+PCl_6^-$. All structurally characterized compounds demonstrated short distances between pyridyl nitrogen and the phosphorus atom. However, the QTAIM analysis did not reveal the presence of appropriate bond critical points (3, –1) for the intramolecular noncovalent interactions N···P in **2**, **4**, and **6**. We theoretically estimated values of the rotation barriers for the pyridyl and Et_2N moieties in **4** using the relaxed potential energy surface scan at the B3LYP/6-31G(d) level of theory. The values of rotation barriers are very close to each other, viz. 13.2 (pyridyl) and 13.0 (Et_2N) kcal/mol.

Introduction

Phosphorus(V) halides are known to form numerous Lewis acid-base adducts with tertiary amines in which phosphorus appears in hexacoordinate state.[1] At the same time, complexation of P^{III} centers with Lewis bases may be complicated by the repulsion of their lone electron pairs. Complex formation is strongly dependent on the value of a positive charge at phosphorus which is determined by the nature of substituents. Equally important is the e-donating properties of a base. However, the particular significance is seen in the polarizability and ionizability of the P–X bond which give rise to the formation of hypervalent phosphorus(III) compounds. Whereas unstable complexes of PCl_3 with trialkylamines were detected only at low temperatures,[2,3] adducts between organoamines and PBr_3 are quite stable at room temperature.[4] Complexes formed in such a way usually have the N–P bond which is close to covalent one, and the P–X bond which is longer than covalent, but do not exceed the sum of van der Waals radii of the elements (Scheme 1).

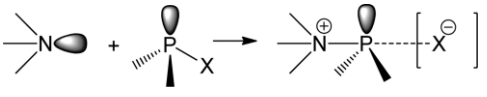

Scheme 1. Interaction of tertiary amines with halophosphines. Square brackets designate the buffer zone for X group which is located between the sum of covalent and the sum of van der Waals radii of the elements.

If ionizability of the P–X bond is not sufficient for moving the X group to the buffer zone (Scheme 1), weak pnictogen bonding takes place (Scheme 2),[5] which has the same nature as related "halogen bonds"[6] or "halcogen bonds"[7,8] arising from σ-hole interactions.[9,10]

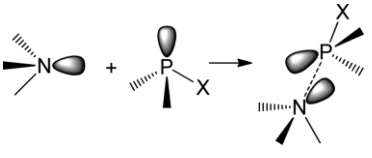

Scheme 2. Pnictogen bonding interaction.

The specific situation takes place, when interaction of donor and acceptor centers is accompanied by charge transfer to another atom. In this case zwitterion is formed (Scheme 3).[11]

On the other hand, electron-delocalizing groups at phosphorus also support the covalent N–P bonding and the formation of zwitterionic compounds based on 3a,6a-diaza-1,4-diphosphapentalene (Scheme 4), whereas R_2C substituents, which do not possess such property, lead to the noncovalent weak N–P interaction.[12]

[a] *G. A. Razuvaev Institute of Organometallic Chemistry, Russian Academy of Sciences*
49 Tropinin str., 603137 Nizhny Novgorod, Russia
E-mail: akornev@iomc.ras.ru
[b] *Saint Petersburg State University,*
7/9 Universitetskaya Nab., 199034 Saint Petersburg, Russia
[c] *Lobachevsky State University of Nizhny Novgorod, Chemical Department,*
23 Gagarina Pr., 603950 Nizhny Novgorod, Russia
Supporting information and ORCID(s) from the author(s) for this article are available on the WWW under https://doi.org/10.1002/ejic.201800831.

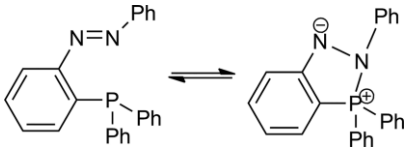

Scheme 3. Intramolecular redox process between phosphino- and azo-functions.

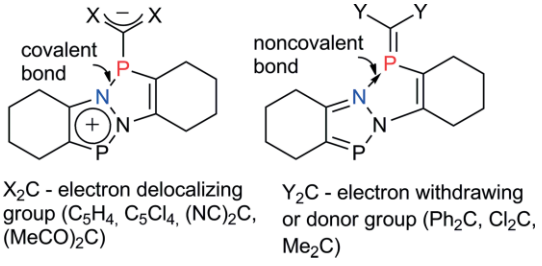

Scheme 4.

2,2′-Azobispyridine (*abpy*) as formally derived from the ubiquitous 2,2′-bipyridine ligand is now known to form a variety of complexes. The structurally identified alternatives for *abpy* metallic complexes include mainly mono- and dinuclear coordinations **I** and **II**, with five-membered chelate ring formation,[13,14] while coordination only by the pyridine group (**III**)[15] and tridentate coordination (**IV**)[16,17] are rarely observed (Scheme 5).

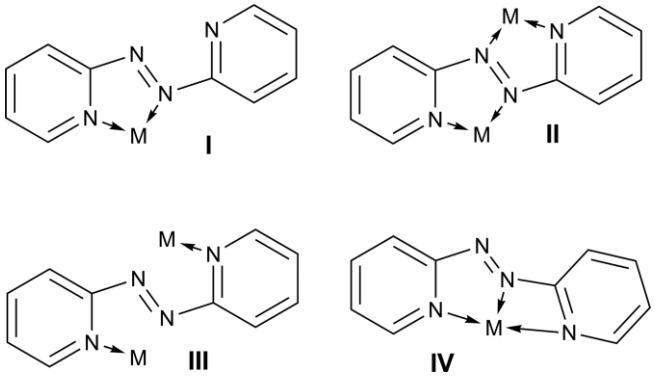

Scheme 5. Coordination modes of 2, 2′-azobispyridyl ligand.

The majority of mononuclear species (**I**) may be described as complexes of unreduced *abpy*^{0} containing N=N bonds in the range 1.25–1.30 Å. Nevertheless, in several complexes (Ru, Os) 2,2′-azobispyridyl exists as an anion-radical displaying the elongated N–N bond (1.34–1.37 Å).[18–20]

With reference to complexes of *abpy* with PCl_3, the resulting oxidation state of phosphorus and the structure of the adduct are not obvious (Scheme 6).

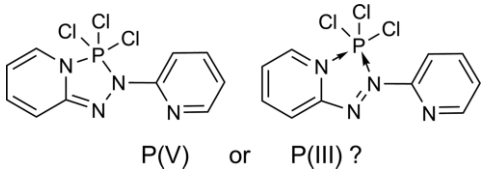

Scheme 6. Two possible adducts of *abpy* with PCl_3.

Following our interest in the chemistry of hypervalent phosphorus(III) compounds,[21–24] we have studied the reaction of 2,2′-azobispyridine and its reduced form (2,2′-hydrazobispyridine, *hbpy*) with PCl_3. An open question also concerns the stability of hypervalent phosphorus compounds **A** and **A′** depicted in Scheme 7, which are analogs of phenylpyrazol-based hypervalent phosphorus compounds (**B**, **B′**) reported previously:[21]

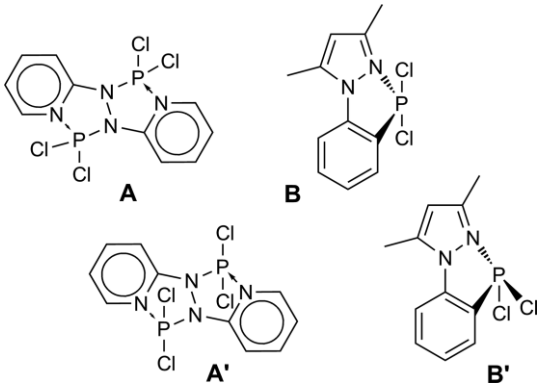

Scheme 7. Possible isomers of *abpy*-based hypervalent phosphorus compounds (**A**, **A′**) and previously reported phenylpyrazole-based analogs (**B**, **B′**).[21]

Results and Discussion

Reaction of PCl_3 with 2,2′-Azobispyridine (abpy)

A sample of 2,2′-azobispyridine was allowed to react with an excess of PCl_3 in toluene or dichloromethane at room temperature overnight. The ^{31}P NMR spectrum of the reaction mixture demonstrates a weak signal at –92.9 ppm which is in the field, typical for cyclic compounds containing phosphorus(V) atom in Cl_3N_2 surrounding.[25] Cooling of the reaction mixture or solvent removal lead to the loss of solubility of the product in organic solvents (THF, Et_2O, PhMe, CH_2Cl_2). Light-brown non-crystalline solid has elemental composition corresponded to *abpy*/PCl_3 = 1:1 ratio. Anaerobic hydrolysis of the *abpy*-PCl_3 adduct in water-base media gave 2,2′-hydrazobispyridine (Py-NHNH-Py, *hbpy*) that confirms the redox reaction between *abpy* and phosphorus trichloride. A similar work-up procedure with methanol yielded *hbpy(HCl)*$_2$ together with trimethyl phosphate, $(MeO)_3PO$, according to the ^{31}P spectrum (Scheme 8).

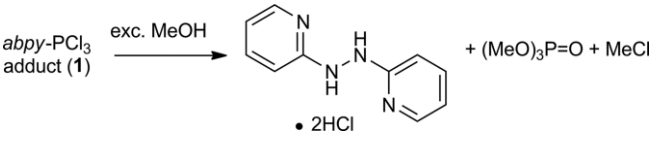

Scheme 8. Methanolysis of abpy-PCl_3 adduct (**1**).

Raman Spectroscopy confirms that azo-bispyridine is reduced in the reaction with PCl_3 since the band 1300 cm^{-1} (N=N, *abpy*) is absent in the product.

Geometry optimization for the asumed *abpy*-PCl_3 adduct at the B3LYP/6-31G(d) level of theory results in the structure **1** as shown in Figure 1.

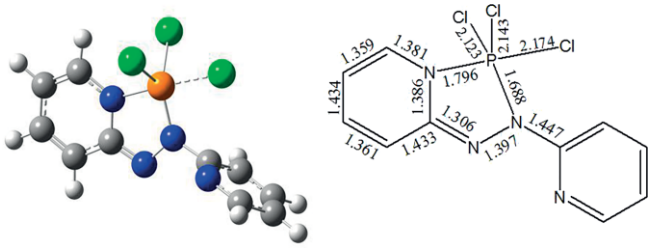

Figure 1. Equilibrium optimized structure of the *abpy*-PCl_3 adduct (**1**) at the B3LYP/6-31G(d) level of theory and its graphic formula with selected bond lengths in Å.

The length of nitrogen–nitrogen bond in **1** (1.397 Å) testified to its single bond character whereas the neighboring C=N bond in the five-membered ring (1.306 Å) has a double bond character.

The phosphorus atom in **1** has a trigonal-bipyramidal environment in which one of the chlorine atom and the nitrogen atom of the "former" pyridine ring occupy axial positions. Thus, calculated structure may be represented as a pentavalent phosphorus compound with reduced *abpy* backbone.

Let's notice, that related phosphorus(III)-containing 2-pyridylazo-species (Scheme 9) undergo intramolecular oxidative addition to form compounds of pentavalent phosphorus.[26]

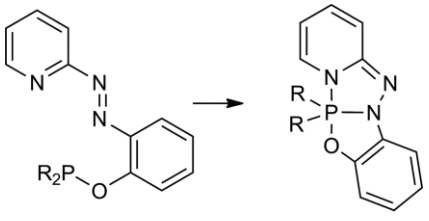

Scheme 9. Intramolecular oxidative addition of phosphorus(III) to azopyridine fragment.[25]

Despite all received indirect data, *abpy*-PCl_3 adduct **1** cannot be assigned to the individual molecular compound. More probably, this is coordination polymer having irregular structure with multiple close intermolecular contacts P–Cl, Cl–Cl, N–P. The widened absorption bands in the IR spectrum confirm this assumption. Nevertheless, oxidation of phosphorus atom in PCl_3 and the corresponding reduction of *abpy* at their interaction were established beyond any doubt.

Reactions of PCl_3 with 2,2′-Hydrazobispyridine (hbpy) and Its Derivatives

Solutions of 2,2′-hydrazobispyridine and PCl_3 in THF after mixing gave abundant pale-yellow precipitate, containing all products of the reaction. By repeated recrystallization from different solvents we succeeded in separating only 15 % of pure phosphorus-containing product **2** according to Scheme 10.

Using triethylamine as an HCl abstractor allowed increasing the yield of **2** up to 25 %. No other phosphorus-containing products were found in these reactions. Low preparative yields of **2** are caused by difficulty in separation from byproducts (hydrochlorides).

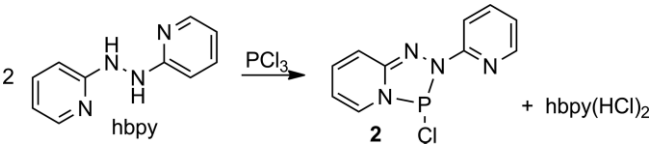

Scheme 10. Reaction of 2,2′-hydrazobispyridine with PCl_3.

The structure of **2** was determined by X-ray crystallographic analysis (Figure 2). Crystal data and some details of the data collection and refinement are given in Table S1 (Supporting Information).

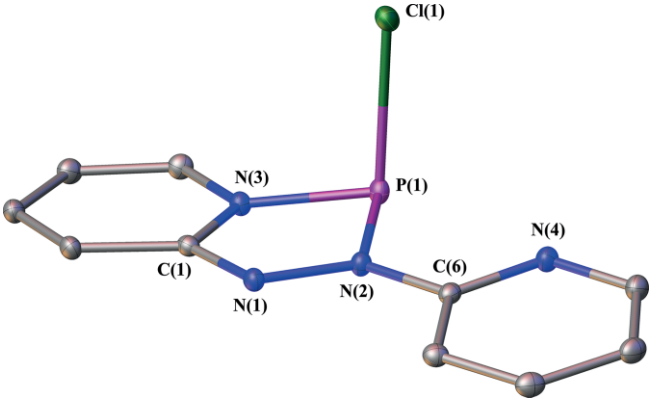

Figure 2. Molecular structure of **2** together with the atomic numbering system. Hydrogen atoms have been omitted for clarity. Thermal ellipsoids are drawn at 30 % probability. Selected bond lengths [Å] and angles [°]: P(1)–N(2) 1.6839(8), P(1)–N(3) 1.7056(8), P(1)–Cl(1) 2.2247(3), N(3)–C(1) 1.3992(11), C(1)–N(1) 1.3058(12), N(1)–N(2) 1.3986(11), N(2)–C(6) 1.4008(11); N(2)–P(1)–N(3) 85.64(4), N(2)–P(1)–Cl(1) 102.51(3), N(3)–P(1)–Cl(1) 99.54(3), P(1)–N(3)–C(1) 112.53(6), N(3)–C(1)–N(1) 115.57(8), C(1)–N(1)–N(2) 106.30(7), N(1)–N(2)–P(1) 118.44(6), N(1)–N(2)–C(6) 119.14(7).

Complex **2** is chiral, and two pairs of enantiomers cocrystallize in the unit cell. The phosphorus atom P(1) in **2** exhibits a pyramidal geometry. The length of the P(1)–Cl(1) bond, 2.2247(3) Å, is in accordance with the P–Cl bond lengths in related 1,3,2-diazaphospholidines.[27,28] Five-membered heterocycle in **2** is not planar, but nitrogen atoms N(1) and N(2) lie in the plane of the annelated six-membered heterocycle, whereas deviation of the phosphorus atom from this plane is 0.23 Å. The nitrogen–nitrogen bond length in **2** [1.399(2) Å] corresponds to the single N–N bond, whereas the neighboring N(1)–C(1) bond, 1.306(2) Å, is of the double bond character [compare to the single bond N(2)–C(6) of 1.401(2) Å]. The pyridine ring after coordination to phosphorus partly losses its aromaticity and demonstrates appreciable distinctions between alternating bonds. The crystal packing analysis of **2** revealed intermolecular H···Cl and H···N interactions, which are less or close to the sum of the van der Waals radii of the elements. Part of the chain is depicted in Figure S1 (Supporting information).

The $^{31}P\{^1H\}$ NMR spectrum of **2** in pyridine showed a single resonance at δ = 115.0 ppm. Measuring of NMR spectra in common organic solvents is unavailable because of very poor solubility of **2**.

Reactions of Dilithium Salt of 2,2′-Hydrazobispyridine with PCl_3 and $(Et_2N)_2PCl$

We attempted to synthesize hypervalent phosphorus derivatives of *abpy* (**A** and **A′**, Scheme 7) using dilithiation of *hbpy* followed by the reaction with PCl_3. However, no individual products were formed in this process. Meanwhile, interaction of dilithium salt of *hbpy* (**3**) with $(Et_2N)_2PCl$ unexpectedly gave compound **4**, containing only one phosphorus atom incorporated into *abpy* backbone (Scheme 11).

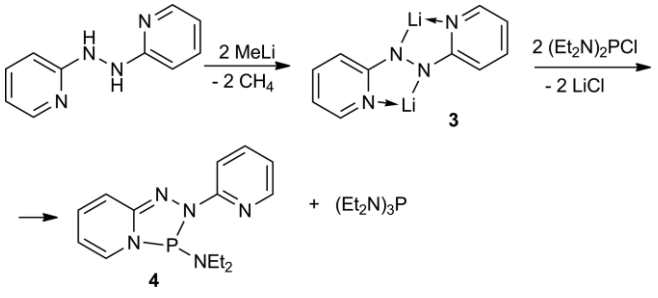

Scheme 11.

The ^{31}P NMR spectrum of **4** showed a single resonance at δ = 82.9 ppm. The second phosphorus-containing product found in this reaction was tris(dimethylamino)phosphine, showing a single resonance at δ = 118.3 ppm in the ^{31}P NMR spectrum.

The structure of **4** was proven by X-ray analysis (Figure 3). Crystal data and some details of the data collection and refinement are given in Table S1 (Supporting Information).

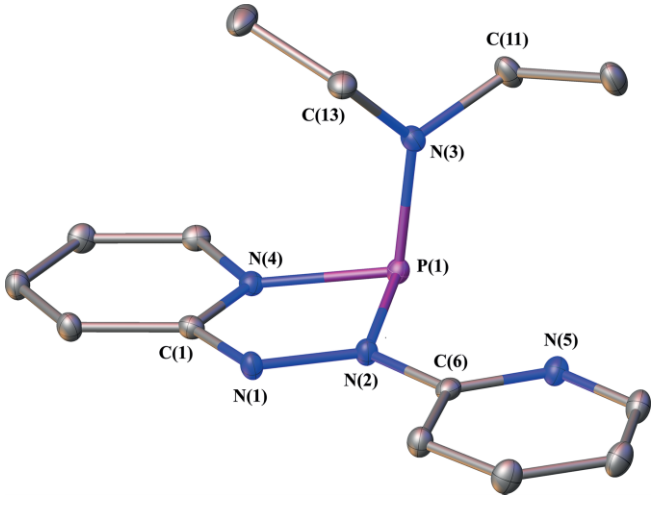

Figure 3. Molecular structure of **4** together with the atomic numbering system. Hydrogen atoms have been omitted for clarity. Thermal ellipsoids are drawn at 30 % probability. Selected bond lengths [Å] and angles [°]: P(1)–N(3) 1.656(2), P(1)–N(2) 1.739(2), P(1)–N(4) 1.758(2), N(4)–C(1) 1.396(2), C(1)–N(1) 1.298(2), N(1)–N(2) 1.412(2), N(2)–C(6) 1.384(2), N(3)–C(13) 1.467(2), N(3)–C(11) 1.468(2); N(3)–P(1)–N(2) 106.36(5), N(3)–P(1)–N(4) 103.74(5), N(2)–P(1)–N(4) 83.19(5), P(1)–N(4)–C(1) 113.41(8), N(4)–C(1)–N(1) 116.30(2), C(1)–N(1)–N(2) 106.55(9), N(1)–N(2)–P(1) 118.63(7), N(1)–N(2)–C(6) 117.57(9), P(1)–N(2)–C(6) 122.99(8), C(13)–N(3)–C(11) 116.81(10), C(13)–N(3)–P(1) 124.78(8), C(11)–N(3)–P(1) 118.26(8).

Complex **4** is chiral, and two pairs of enantiomers cocrystallize in the unit cell. According to the X-ray data, the phosphorus atom in **4** has a pyramidal configuration. The P(1)–N(3) bond length [1.656(2) Å] is in the range characteristic of P–N single bonds of phosphinoamines[29] but noticeably shorter then endocyclic P(1)–N(2) 1.739(2) Å and P(1)–N(4) 1.758(2) Å bonds in the five-membered heterocycle of **4**. At the same time, the sum of angles around the N(3) atom is close to 360° showing its trigonal-planar environment. This phenomenon has already been observed and discussed for related 2-amino-1,3,2-diazaphospholenes and triaminophosphines,[30,31] and may be assigned, most likely, to the necessity and possibility to extinguish the big positive charge at the phosphorus atom more effectively.

Exploring the reaction mechanism has shown that extrusion of $(Et_2N)_3P$ is observed only after addition of the second equivalent of $(Et_2N)_2PCl$ to dilithium salt of *hbpy* (**3**), whereas addition of the first equivalent results in the formation of an intermediate **5** (Scheme 12).

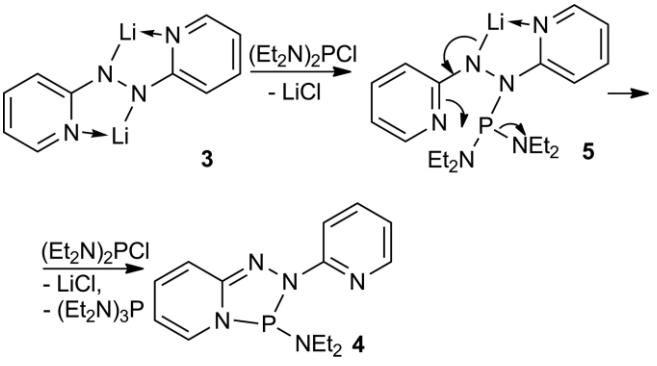

Scheme 12.

Compound **5** shows two close and broadened resonances in the ^{31}P NMR spectrum at δ = 111.0 and 113.3 ppm, which testify, obviously, to the existence of a couple of slightly different coordination modes for monolithium derivative.

It was found that the diethylamido group in **4** may be easily replaced by halogen (Cl, Br) after addition of PCl_3 or PBr_3 respectively (Scheme 13).

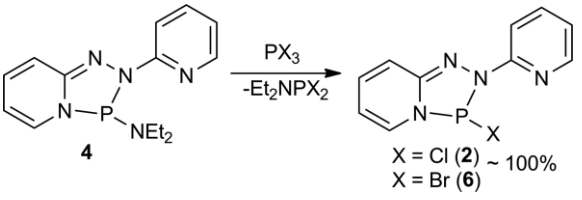

Scheme 13.

The structure of **6** determined by X-ray crystallographic analysis shows close similarity to the chloro-analog **2** (Figure S2 and Table S1 in Supporting information). The molecule **6** is also chiral like **2** and **4**, and two pairs of enantiomers cocrystallize in the unit cell. The crystal packing analysis of **6** revealed intermolecular H···Br and H···N interactions, which are less or close to the sum of the van der Waals radii of the elements. Part of the chain is depicted in Figure S3 in Supporting information.

Considering solid-state crystal structures of complexes **2**, **4**, and **6**, it was noticed, that the nitrogen atom in the pyridyl fragment turns to the phosphorus atom in all cases. Furthermore, the observed distances N···P (2.827, 2.912, 2.824 Å for **2**, **4**, and **6** respectively) are significantly shorter than the sum of van der Waals radii for appropriate atoms (3.35 Å). Thus, in addition to structural analysis, a detailed computational study is desirable.

Computational Study

In order to confirm or deny the hypothesis on the existence of these noncovalent interactions in **2**, **4**, and **6**, we carried out DFT calculations at the M06-2X/6-311++G(d,p) level of theory and performed topological analysis of the electron density distribution within the framework of Bader's theory (QTAIM method).[32] This approach has already been successfully used by us upon studies of different noncovalent interactions (viz. hydrogen, halogen and chalcogen bonding, metallophilic interactions, stacking) in various organic, organometallic, and coordination compounds.[33–37] The QTAIM analysis did not reveal the presence of appropriate bond critical points (3, –1) for the intramolecular noncovalent interactions N···P in **2**, **4**, and **6**, and negligible values of the Wiberg bond indices for these contacts (viz. 0.03–0.04), computed by using the natural bond orbital (NBO) partitioning scheme[38] additionally confirm this observation. The molecular graph from QTAIM analysis of **4** is presented in Figure 4. The contour line diagram of the Laplacian distribution $\nabla^2\rho(\mathbf{r})$, bond paths, and selected zero-flux surfaces as well as isosurface from the reduced density gradient (RDG) analysis[39] of **4** are shown in Figure 5.

In order to explain similar and stable orientation of the pyridyl fragment relative to the phosphorus atom in **2** and **4**, in the absence of noncovalent interaction we performed a geometry optimization for the rotation isomers **2′** and **4′** at the B3LYP/6-31G(d) level of theory (Scheme 14).

It was found that the optimized geometries of **2′** and **4′** correspond to energy minima, as indicated by frequency computations. Molecules **2** and **4** are favored by 7.7 and 8.7 kcal/mol respectively, compared to their rotation isomers **2′** and **4′**. This result may be explained simply by Coulomb attraction in one case (between negatively charged nitrogen and positively charged phosphorus atoms) and Coulomb repulsion in other case (between negatively charged nitrogen atoms), the Mulliken charge distribution in complexes **2**, **2′**, **4**, **4′** is shown in Figure S4 (Supporting information).

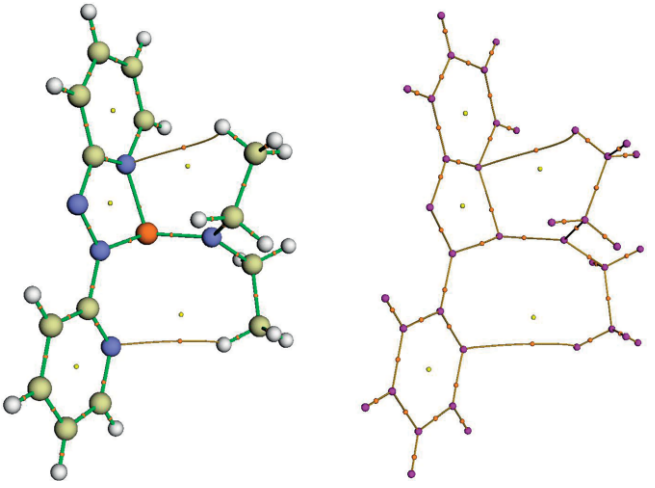

Figure 4. Molecular graph from QTAIM analysis of **4**. The Poincare–Hopf relationship was satisfied, thus all critical points have been found. Bond critical points (3, –1) are shown in orange, nuclear critical points (3, –3) – in violet, ring critical points (3, +1) – in yellow.

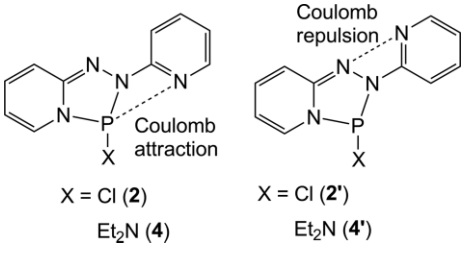

Scheme 14.

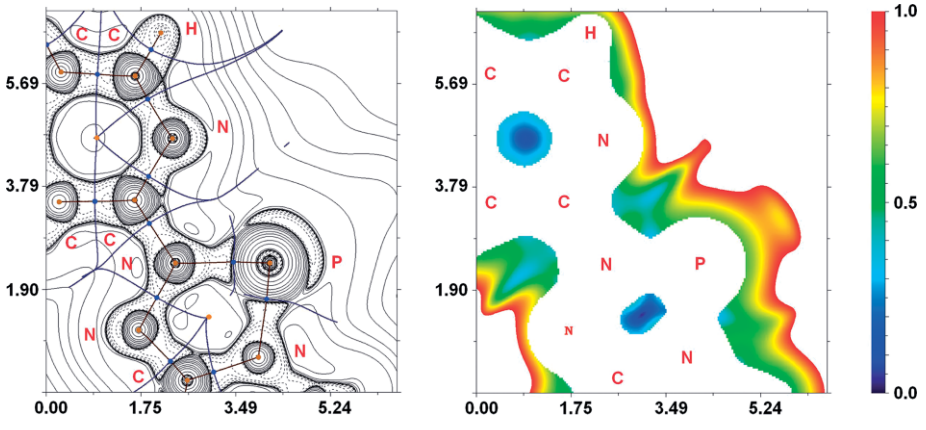

Figure 5. Contour line diagram of the Laplacian distribution $\nabla^2\rho(\mathbf{r})$, bond paths and selected zero-flux surfaces (left) and RDG isosurface (right) referring to the absence of any intramolecular noncovalent interactions N···P in **4**. Bond critical points (3, –1) are shown in blue, nuclear critical points (3, –3) – in pale brown, ring critical points (3, +1) – in orange. Length units: Å, RDG isosurface values are given in Hartree.

We theoretically estimated values of the rotation barriers for the pyridyl and Et_2N moieties in **4** using the relaxed potential energy surface scan at the B3LYP/6-31G(d) level of theory. Based on the obtained equilibrium geometry of **4**, we define appropriate dihedral angles N–C–N–P and C–N–P–N, respectively, to be scanned in the range of 180° by increments of 5°, assuming that the energy barriers associated with the rotation by these dihedral angles can be estimated as the difference between the obtained minimum and maximum values of the calculated total energies. The values of rotation barriers calculated by this technique are relatively small and very close to each other, viz. 13.2 (pyridyl) and 13.0 (Et_2N) kcal/mol.

We performed also a geometry optimization and frequency calculation at the B3LYP/6-31G(d) level of theory for the structures **A** and **A′** (Scheme 7). It was shown that **A** and **A′** have planar abpy-backbones (Figure S5, Supported Information). It should be noticed, however, that the frequency calculation found one imaginary frequency for **A′**. This indicated that we had not found a minimum but rather a first-order saddle point on the potential energy surface.

Interaction of 2 and 4 with Lewis Acids ($SiCl_4$ and PCl_5)

Since molecules **2** and **4** contain Lewis-base centers we tried to elucidate their further coordination activity. Whereas chloro-substituted triazaphospholene **2** does not react with silicon tetrachloride, diethylamino-derivative **4** easily forms adduct **7** by coordination of two nitrogen atoms to silicon (Scheme 15). It should be noticed that cleavage of N–P bonds by $SiCl_4$ was not observed.

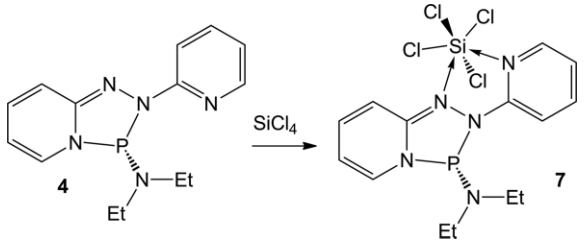

Scheme 15.

The ^{31}P NMR spectrum of **7** shows a single resonance at δ = 75.0 ppm, high field shifted by ca. 7 ppm as compared to **4**.

A single-crystal X-ray diffraction study of **7** shows $SiCl_4$ molecule is incorporated into **4** with the formation of the chelate five-membered heterocycle (Figure 6, Table S1). The hypercoordinate silicon atom appears in a slightly distorted octahedral environment where two chlorine atoms occupy axial positions and other two chlorine atoms lie in the equatorial plane together with nitrogen atoms N(2) and N(3). The Si–Cl bond lengths are comparable to those of silicon tetrachloride complexes with nitrogen bases.[40,41] The silicon atom forms shorter bond with the nitrogen atom of the five-membered ring [Si(1)–N(2) 1.8749(9) Å] compared to the Py→Si coordination [Si(1)–N(3) 1.9462(9) Å]. It is remarkable, the Et_2N-group is more tightly bonded to the phosphorus atom in adduct **7** [1.641(2) Å] in comparison with the free ligand **4** [1.656(2) Å]. Obviously, its donor properties play a crucial role in the formation of donor–acceptor complex **7**, since chloro-derivative **2** does not form such complex.

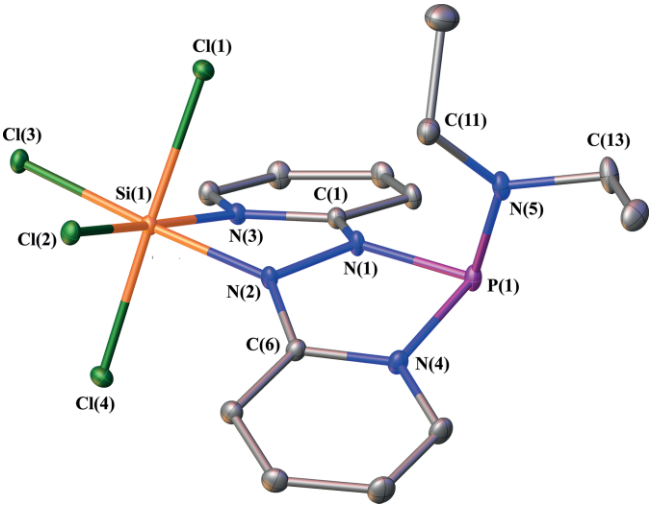

Figure 6. Molecular structure of **7** together with the atomic numbering system. Hydrogen atoms and the solvate molecule of THF have been omitted for clarity. Thermal ellipsoids are drawn at 30 % probability. Selected bond lengths [Å] and angles [°]: Si(1)–N(2) 1.8749(9), Si(1)–N(3) 1.9462(9), Si(1)–Cl(1) 2.2384(4), Si(1)–Cl(2) 2.1591(4), Si(1)–Cl(3) 2.1681(4), Si(1)–Cl(4) 2.1816(4), P(1)–N(5) 1.6409(11), P(1)–N(1) 1.7293(9), P(1)–N(4) 1.7909(10), N(2)–C(6) 1.3343(13), N(2)–N(1) 1.4138(12), N(1)–C(1) 1.3643(13), N(5)–C(13) 1.4721(14), N(5)–C(11) 1.4689(15); Cl(4)–Si(1)–Cl(1) 177.30(2), N(3)–Si(1)–Cl(2) 171.63(3), N(2)–Si(1)–Cl(3) 173.70(3), Cl(2)–Si(1)–Cl(3) 93.00(2), N(2)–Si(1)–N(3) 79.91(4), N(5)–P(1)–N(1) 104.02(5), N(5)–P(1)–N(4) 104.06(5), N(1)–P(1)–N(4) 83.17(4), C(6)–N(2)–N(1) 108.98(8), C(1)–N(1)–N(2) 111.97(8), C(1)–N(1)–P(1) 126.49(7), N(2)–N(1)–P(1) 117.39(7), C(13)–N(5)–C(11) 117.16(10), C(13)–N(5)–P(1) 115.84(9), C(11)–N(5)–P(1) 125.17(8).

It should be noted also, that coordination of $SiCl_4$ causes notable redistribution of bond lengths in five-membered ring. The bonding of phosphorus with the nitrogen atom of the pyridyl fragment is weakened [1.758(2) Å in **4** and 1.791(2) Å in **7**] together with weakening of π-character of the C=N bond [1.298(2) Å in **4** and 1.334(2) Å in **7**]. The crystal structure of **7** reveals multiple H···Cl and C···Cl intermolecular short contacts; Cl···Cl short contacts were not observed in contrast to related $SiCl_4$(phen) molecule.[40]

Since the five-membered ring in **2** has the labile halogen atom, we tried to fix the aromatic 6π-electron triazaphosphalene cation by addition of PCl_5 (Scheme 16).

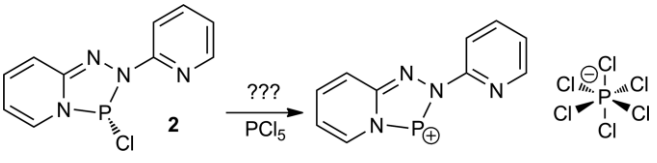

Scheme 16.

The experiment showed, however, that redox process took place with the formation of tetrahedral phosphorus(V) complex **8** and liberation of phosphorus trichloride (Scheme 17).

Since compound **8** has the salt-like nature and completely insoluble in common organic solvents, its NMR spectra were unavailable. However, mother liquor of the reaction mixture

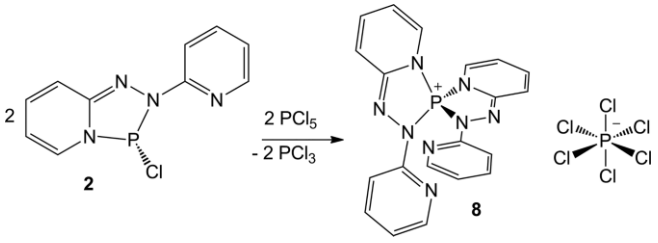

Scheme 17.

contained three single resonances. Two of them we assigned to PCl_3 (δ =219.6 ppm) and cationic part of **8** (δ =4.2 ppm). The third signal (–220.7 ppm) may be assigned to the adduct of PCl_5 with nitrogen base, not to the hexachlorophosphate anion (–280 to –310 ppm).[1] Crystals of **8** suitable for X-ray analysis were grown from the reaction mixture at room temperature. Cationic part of complex **8** contains the chiral tetrahedral phosphorus atom; two pairs of enantiomers cocrystallize in the unit cell together with dichloromethane as a solvate molecule. Crystal data and some details of the data collection and refinement are given in Table S1 (Supporting Information); the molecular structure of **8** is depicted in Figure 7. Both five-membered heterocycles in **8** are planar, with the dihedral angle between planes of 89.0°. The crystal structure of **8** revealed the packing arrangement with multiple C···H, C···Cl, H···Cl, and Cl···Cl short contacts.

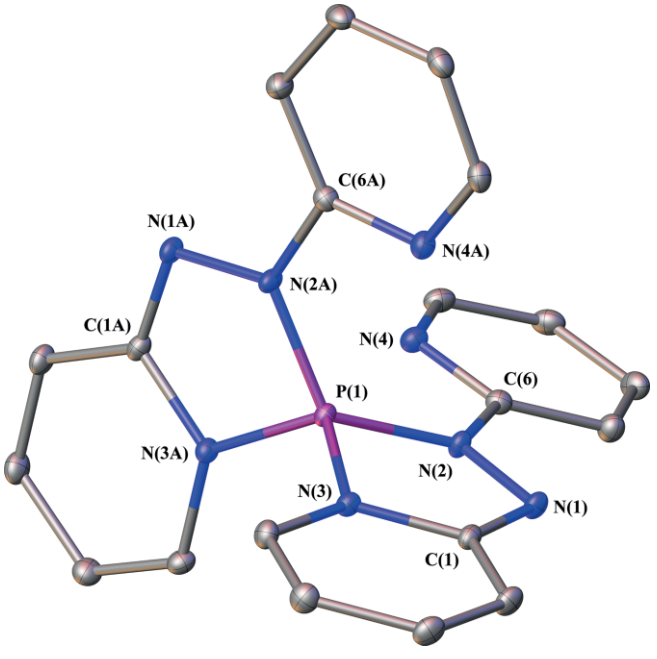

Figure 7. Molecular structure of **8** together with the atomic numbering system. Hydrogen atoms, the anion PCl_6^- and the solvate molecule of CH_2Cl_2 have been omitted for clarity. Thermal ellipsoids are drawn at 30 % probability. Selected bond lengths [Å] and angles [°]: P(1)–N(2) 1.641(2), P(1)–N(3) 1.648(2), N(1)–N(2) 1.404(2), N(1)–C(1) 1.303(2), N(3)–C(1) 1.409(2), N(2)–C(6) 1.413(2); N(2A)–P(1)–N(2) 125.14(11), N(2)–P(1)–N(3) 90.03(7), N(2)–P(1)–N(3A) 120.17(7), N(3A)–P(1)–N(3) 113.80(11).

Comparison of **8** with other *abpy*-containing species was instructive: the tetrahedral phosphorus(V) atom is more tightly bonded to the *abpy* ligand. The N–P bonds in **8** are shorter by approximately 0.05 Å in comparison with **2** and by ≈ 0.1 Å in comparison with diethylamino derivative **4**. Other bond lengths in *abpy* fragments of **2**, **4**, and **8** do not notably differ.

Remarkably, the intramolecular N···P contact N(4)–P(1), 2.764 Å, is clearly shorter than the related distances N···P in **2**, **4** and **6** (2.827, 2.912, 2.824 Å respectively) which has a direct relationship with the charge of the phosphorus atom (Figure S6, Supporting information). It is known that spyrocyclic tetraazophosphonium cations like **8** may be formed by the cycloaddition reactions of 1,3,2-diazaphosphalenes with diaza-1,3-butadienes.[42]

Conclusions

In the present work we have applied 2,2′-azobispyridine (*abpy*) and its reduced form – 2,2′-hydrazobispyridine (*hbpy*) to the phosphorus chemistry. It was shown that PCl_3 reduces *abpy* in dichloromethane or toluene with the formation of the oxidative addition product (1:1). Application of PCl_3 in the reaction with *hbpy* gave $(abpy)^{2-}PCl$ (**2**), containing the 1,2,4,3-triazaphosphole ring. Dilithium salt of *hbpy* gave no individual products in the reaction with PCl_3, but excellent yield of $(abpy)^{2-}PNEt_2$ (**4**) in the reaction with $(Et_2N)_2PCl$. Diethylamido-group in **4** may be easily substituted by Cl or Br atoms in the reaction of **4** with PCl_3 or PBr_3 respectively. $SiCl_4$ and compound **4** in the mixture (1:1) do not demonstrate exchange between the Et_2N group and the Cl atom, but form complex **7** with coordination of silicon by pyridyl- and azo-functions. The donor Et_2N group plays a crucial role in this coordination since Cl-derivative (**2**) does not form complex with $SiCl_4$. We have found that compound **2** reacts with PCl_5 with liberation of PCl_3 and the formation of spirocyclic *ate* complex $[(abpy)^{2-}{}_2P]^+PCl_6^-$. Structural analysis reveals short distances between pyridyl nitrogen and the phosphorus atom in all structurally characterized compounds which may be explained by Coulomb attraction since the QTAIM analysis demonstrated no appropriate bond critical points (3, –1) for the intramolecular noncovalent interactions N···P in **2**, **4**, and **6**. Rotation barriers for the pyridyl and Et_2N groups in **4** were theoretically estimated to be very close to each other [13.2 (pyridyl) and 13.0 (Et_2N) kcal/mol].

Experimental Section

General Procedures: All preparations were performed by using standard Schlenk techniques under dry, oxygen-free dinitrogen or argon. Solvents were distilled from appropriate drying agents immediately prior to use:[43] diethyl ether and THF were dried and distilled from Na/benzophenone, pyridine was distilled from KOH and kept over CaH_2, toluene and hexane were thoroughly dried and distilled from sodium prior to use. Bis(*N*,*N*-diethylamino)chlorophosphine, 2-aminopyridine, PCl_3, PBr_3, and silicon tetrachloride were purchased from Sigma–Aldrich Chemical Co. and distilled before use. For the synthesis of known compounds (2,2′-azobispyridine[44] and 2,2′-hydrazobispyridine[45]) we used modified methods described below.

NMR spectra were recorded on a Bruker DPX-200 and AV-400 spectrometers. IR spectra were recorded with a Perkin–Elmer 577 spec-

trometer from 4000 to 400 cm^{-1} in Nujol or with a Perkin–Elmer FT-IR Spectrometer System 2000 as KBr discs.

X-ray Crystallography: The X-ray diffraction data were collected on a SMART APEX (for **8**) and a Bruker D8 Quest (for **2**, **4**, **6** and **7**) diffractometers (Mo-K_α radiation, ω-scan technique, λ = 0.71073 Å). The intensity data were integrated by SAINT.[46] All structures were solved by direct methods using a dual-space algorithm with the SHELXT program.[47] Refinement of the structures was carried out on F^2_{hkl} using SHELXTL package.[48,49] All non-hydrogen atoms were refined anisotropically. Hydrogen atoms were placed in calculated positions and were refined in the riding model with the exception of those located at the solvate dichloromethane molecule in **8** from a difference Fourier synthesis of electron density and refined isotropically SADABS[50] was used to perform area-detector scaling and absorption corrections. Crystal of **7** contains the solvate molecule of THF. The main crystallographic data and structure refinement details for **2**, **4**, **6**, **7** and **8** are presented in Table S1.

CCDC 1826171 (for **2**), 1826172 (for **4**), 1826173 (for **6**), 1826174 (for **7**), and 1826175 (for **8**) contain the supplementary crystallographic data for this paper. These data can be obtained free of charge from The Cambridge Crystallographic Data Centre.

Details of QTAIM Analysis: The single point calculations based on the experimental X-ray geometries have been carried out at the DFT level of theory using the M06-2X functional[51] (this functional was parameterized for main group elements and specifically developed to describe weak dispersion forces and noncovalent interactions) with the help of Gaussian-09 (see General information in SI) program package. The standard 6-311++G(d,p) basis sets were used for all atoms. The topological analysis of the electron density distribution with the help of the atoms in molecules (QTAIM) method developed by Bader[52] has been performed by using the Multiwfn program (version 3.3.8)[53] The Cartesian atomic coordinates of model species are presented in Table S2 (Supporting Information).

Synthesis

2,2′-Azobispyridine (*abpy*): A solution of 2-aminopyridine (4.70 g, 0.05 mol) in 100 mL of toluene was added to a manganese(IV) oxide (30.43 g, 0.35 mol). The reaction mixture was stirred for 10 days at 115 °C. The solution was filtered and the solvent was removed under vacuum, leaving a deep-red solid. The residual starting 2-aminopyridine was removed from the crude product by sublimation at 57 °C/0.05 Torr. The reddish-brown product was recrystallized from toluene and dried in vacuo. Yield: 1.95 g, 40 %. ^{1}H NMR ($CDCl_3$, 300 K): δ = 8.79 (br. s, 2 H), 8.13–7.87 (m, 4 H), 7.57–7.39 (m, 2 H) ppm. IR (Nujol): $\tilde{\nu}$ = 1578 cm^{-1} (m), 1423 (m), 1263 (w), 1144 (w), 1097 (w), 990 (m), 796 (s), 737 (s), 625 (m), 559 (m), 522 (m) cm^{-1}. MS: *m/z* (%) = 184.3 (20) $[M]^+$, 156.1 (100) $[M - N_2]^+$. $C_{10}H_8N_4$ (184.2): calcd. C 65.21; H, 4.38; found C 65.12; H, 4.43 %.

2,2′-Hydrazobispyridine (*hbpy*): Hydrazine hydrate (13.5 g, 0.27 mol) was added to a solution of *abpy* (0.50 g, 2.71 mmol) in 10 mL of ethanol. The mixture was stirred at 30 °C for 24 h in open flask before crystalline product started to form. The reaction mixture was concentrated up to 3 mL; pale-yellow crystals were separated from the mother liquor, washed with EtOH and dried in vacuo. Yield: 0.32 g, 63.4 %. ^{1}H NMR ([D_8]THF, 300 K): δ = 6.18 [d, ^3J(H,H) = 4.8 Hz, 2 H], 5.84 (br. s, 2 H, NH), 5.56 (t, $^3J_{H,H}$ = 7.8 Hz, 2 H), 4.6–4.9 (m, 4 H) ppm. ^{13}C NMR ([D_8]THF, 50 MHz): δ = 159.3 (s), 146.1 (s), 135.2 (s), 112.3 (s), 103.6 (s) ppm. IR (Nujol): $\tilde{\nu}$ = 3206 cm^{-1} (s), 3155 (s), 3063 (s), 1593 (vs), 1452 (vs), 1432 (vs), 1309 (s), 1279 (m), 1252 (m), 1147 (s), 991 (s), 772 (vs), 732 (vs), 625 (w), 597 wide (w), 510 (m) cm^{-1}. $C_{10}H_{10}N_4$ (186.21): calcd. C 64.50; H, 5.41; found C 64.46; H, 5.45 %.

***Abpy*-PCl_3 Adduct (1):** A solution of PCl_3 (0.93 g, 6.77 mmol) in 10 mL of toluene or CH_2Cl_2 was added to a solution of 2,2′-azobispyridine (0.50 g, 2.71 mmol) in 10 mL of the same solvent. The mixture was kept overnight at room temperature, then solvent was removed in vacuo together with the rest of PCl_3. The product losses solubility after solvent removal and may be washed with pure THF or CH_2Cl_2. The precipitate was filtered off and dried in vacuo. Yield: 1.51 g (94 %). IR (Nujol): $\tilde{\nu}$ = 1642 (m), 1608 (m), 1554 (w), 1528 (w), 1285 (m), 1227 (w), 1163 (m), 1107 (w), 1027 (w), 992 (m), 934 (w), 854 (m), 771 (s), 738 (w), 677 (w), 619 (w), 545 (m), 516 (m). $C_{10}H_8Cl_3N_4P$ (319.96): calcld. C, 37.35; H, 2.51; Cl, 33.08; P, 9.63; found C 37.40; H, 2.47; Cl, 32.95; P, 9.56.

Dilithium Salt of *hbpy* (3): A solution of MeLi in diethyl ether (0.85 M, 1.89 mL, 1.60 mmol) was added to a solution of 2,2′-hydrazobispyridine (0.15 g, 0.80 mmol) in 10 mL of THF at – 70 °C. The mixture immediately turns deep-red. Formation of gas – CH_4 – was detected. Prepared dilithium salt of *hbpy* (**3**) was used *in situ*.

***N,N*-Diethyl-2-(pyridin-2-yl)-[1,2,4,3]triazaphospholo[4,5-*a*]pyridin-3(3*H*)-amine (4):** A solution of $(Et_2N)_2PCl$ (0.34 g, 1.60 mmol) in 3.0 mL of THF was added to the solution of **3** (0.80 mmol) in THF at – 70 °C. The reaction mixture was kept at room temperature overnight. THF was replaced by toluene. The precipitate of LiCl was filtered off and toluene was replaced by hexane. The solution was concentrated; pale-yellow crystals were separated from the mother liquor, washed with hexane and dried in vacuo. Yield: 0.20 g, 89 %. ^{1}H NMR (C_6D_6, 300 K): δ = 8.20 (ddd, *J* = 4.9, 1.8, 0.8 Hz, 1 H), 7.78 (d, *J* = 8.4 Hz, 1 H), 7.24–7.19 (m, 1 H), 6.78 (ddt, *J* = 7.2, 5.0, 1.2 Hz, 1 H), 6.58 (dd, *J* = 9.5, 1.1 Hz, 1 H), 6.4 (ddd, 7.2, 4.9, 1.0 Hz, 1 H), 6.18 (ddt, *J* = 9.5, 6.1, 1.1 Hz, 1 H), 5.34 (ddd, *J* = 7.1, 6.3, 1.1 Hz, 1 H), 2.84 (m, 4 H,CH_2CH_3), 0.78 ppm (t, *J* = 7.1 Hz, 6 H,CH_2CH_3) ppm. ^{13}C NMR (C_6D_6, 50 MHz): δ = 157.63 (d, *J* = 11.0 Hz), 147.65 (d, *J* = 8.0 Hz), 147.25 (s), 137.48 (s), 132.02 (s), 131.58 (s), 130.42 (d, *J* = 1.9 Hz), 115.51–114.73 (m), 109.38 (d, *J* = 1.2 Hz), 105.49 (d, *J* = 7.7 Hz), 40.43 (d, *J* = 18.3 Hz), 14.16 (d, *J* = 3.0 Hz) ppm. ^{31}P NMR (C_6D_6, 81 MHz): δ = 82.9 ppm. IR (Nujol): $\tilde{\nu}$ = 1634 (s), 1604 (m), 1591 (s), 1555 (s), 1525 (m), 1434 (s), 1400 (w), 1345 (s), 1303 (s), 1203 (m), 1175 (m), 1159 (w), 1141 (m), 1059 (m), 1045 (s), 1015 (s), 995 (w), 982 (w), 970 (m), 930 (m), 918 (w), 852 (m), 787 (m), 764 (m), 748 (m), 730 (w), 713 (w), 676 (s), 659 (m), 542 (m), 514 (w). $C_{14}H_{18}N_5P$ (287.30): calcld. C, 58.53; H, 6.31; P, 10.78; found C 58.58; H, 6.27; P, 10.82.

3-Chloro-2-(pyridin-2-yl)-2,3-dihydro-[1,2,4,3]triazaphospholo[4,5-*a*]pyridine (2): 1) An excess of PCl_3 (0.66 g, 4.83 mmol) was added to a solution of **4** (0.23 g, 0.80 mmol) in 20 mL of Et_2O; a yellow crystalline precipitate was formed immediately. The solution was concentrated; crystals were separated from the mother liquor, washed with diethyl ether and dried in vacuo. Yield: 0.19 g, 95 %. ^{31}P NMR (Pyridine, 81 MHz, 243 K): δ = 115.0 ppm. IR (Nujol): $\tilde{\nu}$ = 1639 (m), 1612 (w), 1592 (m), 1568 (w), 1543 (w), 1527 (w), 1446 (s), 1340 (w), 1291 (s), 1259 (w), 1213 (w), 1160 (w), 1146 (w), 1075 (w), 1048 (w), 1033 (wide w), 990 (w), 855 (m), 833 (w), 789 (s), 749 (s), 739 (s), 699 (w), 681 (m), 620 (w), 520 (m). $C_{10}H_8ClN_4P$ (250.62): calcld: C, 47.92; H, 3.22; Cl, 14.15; N, 22.35; P, 12.36; found C 47.89; H, 3.26; Cl, 14.11; P, 12.32.

2) Phosphorus trichloride (0.33 g, 2.4 mmol) was added to the mixture of Et_3N (0.16 g, 1.61 mmol) and *hbpy* (0.15 g, 0.8 mmol) in 100 mL of THF. The plentiful precipitate was formed immediately. The precipitate [mixture of **2** and Et_3N(HCl)] was filtered off and extracted with hot THF. Solubility of **2** in hot THF is slightly better than of Et_3N(HCl) that allowed to separate **2** from the united mother liquors in 25 % yield (0.49 g).

3-Bromo-2-(pyridin-2-yl)-2,3-dihydro-[1,2,4,3]triazaphospholo[4,5-*a*]pyridine (6): An excess of PBr_3 (0.56 g, 2.08 mmol) was added to the solution of **4** (0.1 g, 0.35 mmol) in 20 mL of Et_2O; a yellow crystalline precipitate was formed immediately. The solution was concentrated; precipitate was separated from the mother liquor, washed with diethyl ether and dried in vacuo. Yield: 0.08 g, 79 %. ^{31}P NMR (CH_2Cl_2, 81 MHz, 243 K): δ = 135.5 ppm (br). IR (Nujol): $\tilde{\nu}$ = 1637 (m), 1614 (very w), 1592 (m), 1568 (w), 1539 (w), 1525 (w), 1444 (s), 1339 (w), 1304 (w), 1290 (s), 1263 (w), 1210 (w), 1159 (w), 1144 (w), 1077 (w), 1049 (m), 991 (w), 855 (m), 834 (vw), 788 (s), 751 (s), 743 (s), 700 (w), 683 (m), 621 (w), 518 (m). $C_{10}H_8BrN_4P$ (295.08): calcd. C 40.70; H, 2.73; Br, 27.08; P, 10.50 %; C, 40.67; H, 2.76; Br, 27.03; P, 10.44 %.

Complex of 4 with $SiCl_4$ (7): $SiCl_4$ (0.5 g, 2.94 mmol) was added to the solution of **4** (0.11 g, 0.38 mmol) in 10 mL of THF. The mixture was left at room temperature overnight. The solution was concentrated, orange crystals were filtered, washed with THF and dried in vacuo. Yield: 0.12 g, 68.6 %. ^{31}P NMR (THF, 81 MHz, 243 K): δ = 75.1 ppm. IR (Nujol): $\tilde{\nu}$ = 1631 (s), 1617 (s), 1566 (w), 1508 (s), 1352 (m), 1306 (w), 1267 (w), 1204 (w), 1160 (m), 1131 (w), 1092 (w), 1036 (w), 1017 (s), 1001 (w), 947 (w), 892 (m), 788 (w), 767 (s), 757 (s), 734 (m), 687 (w), 669 (w), 659 (w), 601 (w), 544 (w), 472 (vs), 456 (vs). Chemical Formula: $C_{18}H_{26}Cl_4N_5OPSi$ (529.30): calcd. C 40.84; H, 4.95; Cl, 26.79; found C 40.80; H, 5.02; Cl, 26.83 %.

(*R*)-2,2′-Di(pyridin-2-yl)-2*H*,2′H-3,3′-spirobi[[1,2,4,3]triazaphospholo[4,5-*a*]pyridin]-3-ium Hexachlorophosphate (8): A solution of PCl_5 (0.09 g, 0.46 mmol) in CH_2Cl_2 (10 mL) was added to the suspension of **2** (0.13 g, 0.52 mmol) in 5 mL of the same solvent. The mixture was left at room temperature overnight. The solution was decanted and concentrated. Yellow crystals were filtered, washed with CH_2Cl_2 and dried in vacuo. Yield: 0.06 g, 34.6 %. IR (Nujol): $\tilde{\nu}$ = 1643 (m), 1620 (w), 1599 (m), 1571 (w), 1553 (m), 1530 (w), 1449 (s), 1339 (w), 1305 (w), 1290 (m), 1255 (w), 1182 (m), 1171 (w), 1148 (w), 1132 (w), 1101 (w), 1058 (w), 994 (very w), 852 (m), 807 (w), 773 (m), 749 (m), 738 (m), 679 (w), 563 (w), 491 (w), 481 (w), 445 (s). $C_{21}H_{18}Cl_8N_8P_2$ (727.97): calcd. C 34.65; H, 2.49; Cl, 38.96; P, 8.51; found C 34.60; H, 2.53; Cl, 30.00; P, 8.46 %.

Acknowledgments

The work was performed using the instrumental base of the Analytical Center of the G. A. Razuvaev Institute of Organometallic Chemistry, Russian Academy of Sciences and supported by the Russian Science Foundation (grant no. 14-13-01015-P). Alexander S. Novikov is grateful to Russian Foundation for Basic Research for support (project No. 16-33-60063).

Keywords: Phosphorus heterocycles · Azo compounds · Noncovalent interactions · Azaphospholes · 2,2′-Azobispyridine

[1] C. Y. Wong, D. K. Kennepohl, R. G. Cavell, *Chem. Rev.* **1996**, *96*, 1917–1952.
[2] W. R. Trost, *Can. J. Chem.* **1954**, *32*, 356–361.
[3] R. R. Holmes, *J. Phys. Chem.* **1960**, *64*, 1295–1299.
[4] G. Müller, J. Brand, S. E. Jetter, *Z. Naturforsch. B* **2001**, *56*, 1163–1171.
[5] S. Zahn, R. Frank, E. Hey-Hawkins, B. Kirchner, *Chem. Eur. J.* **2011**, *17*, 6034–6038.
[6] G. Cavallo, P. Metrangolo, R. Milani, T. Pilati, A. Priimagi, G. Resnati, G. Terraneo, *Chem. Rev.* **2016**, *116*, 2478–2601.
[7] K. T. Mahmudov, M. N. Kopylovich, M. Fátima, C. Guedes da Silva, A. J. L. Pombeiro, *Dalton Trans.* **2017**, *46*, 10121–10138.
[8] D. J. Pascoe, K. B. Ling, S. L. Cockroft, *J. Am. Chem. Soc.* **2017**, *139*, 15160–15167.
[9] H. Wang, W. Wang, Wei J. Jin, *Chem. Rev.* **2016**, *116*, 5072–5104.
[10] T. Clark, *Faraday Discuss.* **2017**, *203*, 9–27.
[11] M. Yamamura, N. Kano, T. Kawashima, *J. Am. Chem. Soc.* **2005**, *127*, 11954–11955.
[12] A. N. Kornev, V. E. Galperin, Y. S. Panova, A. V. Arapova, E. V. Baranov, G. K. Fukin, G. A. Abakumov, *Z. Anorg. Allg. Chem.* **2017**, *643*, 1208–1214.
[13] W. Kaim, *Coord. Chem. Rev.* **2001**, *219–221*, 463–488.
[14] D. A. Baldwin, A. B. P. Lever, R. V. Parish, *Inorg. Chem.* **1969**, *8*, 107–115.
[15] M. Bardají, M. Barrio, P. Espine, *Dalton Trans.* **2011**, *40*, 2570–2577.
[16] M. Camalli, F. Caruso, G. Mattogno, E. Rivarola, *Inorg. Chim. Acta* **1990**, *170*, 225–231.
[17] H. Tsurugi, H. Tanahashi, H. Nishiyama, W. Fegler, T. Saito, A. Sauer, J. Okuda, K. Mashima, *J. Am. Chem. Soc.* **2013**, *135*, 5986–5989.
[18] A. Das, T. M. Scherer, S. M. Mobin, W. Kaim, G. K. Lahiri, *Chem. Eur. J.* **2012**, *18*, 11007–11018.
[19] K. Pramanik, M. Shivakumar, P. Ghosh, A. Chakravorty, *Inorg. Chem.* **2000**, *39*, 195–199.
[20] S. Sengupta, I. Chakraborty, A. Chakravorty, *Eur. J. Inorg. Chem.* **2003**, 1157–1160.
[21] A. N. Kornev, V. V. Sushev, Y. S. Panova, N. V. Zolotareva, E. V. Baranov, G. K. Fukin, G. A. Abakumov, *Eur. J. Inorg. Chem.* **2015**, 2057–2066.
[22] A. N. Kornev, N. V. Zolotareva, V. V. Sushev, A. V. Cherkasov, G. A. Abakumov, *Mendeleev Commun.* **2015**, *25*, 236–238.
[23] A. N. Kornev, *Phosphorus Sulfur Silicon Relat. Elem.* **2016**, *191*, 1497–1500.
[24] A. N. Kornev, V. V. Sushev, Y. S. Panova, O. V. Lukoyanova, S. Yu. Ketkov, E. V. Baranov, G. K. Fukin, M. A. Lopatin, Y. G. Budnikova, G. A. Abakumov, *Inorg. Chem.* **2014**, *53*, 3243–3252.
[25] A. Schmidpeter, Y. Tautz, F. Schreiber, *Z. Anorg. Allg. Chem.* **1981**, *475*, 211–231.
[26] A. Schmidpeter, J. H. Weinmaier, *Angew. Chem. Int. Ed. Engl.* **1977**, *16*, 865–866; *Angew. Chem.* **1977**, *89*, 903.
[27] S. Burck, D. Gudat, K. Nättinen, M. Nieger, M. Niemeyer, D. Schmid, *Eur. J. Inorg. Chem.* **2007**, 5112–5119.
[28] O. Puntigam, I. Hajdók, M. Nieger, M. Niemeyer, S. Strobel, D. Gudat, *Z. Anorg. Allg. Chem.* **2011**, *637*, 988–994.
[29] Z. Fei, P. J. Dyson, *Coord. Chem. Rev.* **2005**, *249*, 2056–2074.
[30] Z. Benkő, S. Burck, D. Gudat, M. Nieger, L. Nyulászi, N. Shorea, *Dalton Trans.* **2008**, 4937–4945.
[31] S. Burck, D. Gudat, F. Lissner, K. Nättinen, M. Nieger, T. Schleid, *Z. Anorg. Allg. Chem.* **2005**, *631*, 2738–2745.
[32] R. F. W. Bader, *Chem. Rev.* **1991**, *91*, 893–928.
[33] T. V. Serebryanskaya, A. S. Novikov, P. V. Gushchin, M. Haukka, R. E. Asfin, P. M. Tolstoy, V. Yu. Kukushkin, *Phys. Chem. Chem. Phys.* **2016**, *18*, 14104–14112.
[34] A. S. Mikherdov, M. A. Kinzhalov, A. S. Novikov, V. P. Boyarskiy, I. A. Boyarskaya, D. V. Dar'in, G. L. Starova, V. Yu. Kukushkin, *J. Am. Chem. Soc.* **2016**, *138*, 14129–14137.
[35] S. A. Adonin, I. D. Gorokh, A. S. Novikov, P. A. Abramov, M. N. Sokolov, V. P. Fedin, *Chem. Eur. J.* **2017**, *23*, 15612–15616.
[36] D. M. Ivanov, Y. V. Kirina, A. S. Novikov, G. L. Starova, V. Y. Kukushkin, *J. Mol. Struct.* **2018**, *1104*, 19–23.
[37] Z. M. Bikbaeva, A. S. Novikov, V. V. Suslonov, N. A. Bokach, V. Yu. Kukushkin, *Dalton Trans.* **2017**, *46*, 10090–10101.
[38] E. D. Glendening, C. R. Landis, F. Weinhold, *Wiley Interdiscip. Rev.: Comput. Mol. Sci.* **2012**, *2*, 1–42.
[39] E. R. Johnson, S. Keinan, P. Mori-Sánchez, J. Contreras-García, A. J. Cohen, W. Yang, *J. Am. Chem. Soc.* **2010**, *132*, 6498–6506.
[40] G. W. Fester, J. Eckstein, D. Gerlach, J. Wagler, E. Brendler, E. Kroke, *Inorg. Chem.* **2010**, *49*, 2667–2673.
[41] O. Bechstein, B. Ziemer, D. Hass, S. I. Trojanov, V. B. Rybakov, G. N. Maso, *Z. Anorg. Allg. Chem.* **1990**, *582*, 211–216.
[42] C. A. Caputo, J. T. Price, M. C. Jennings, R. McDonald, N. D. Jones, *Dalton Trans.* **2008**, 3461–3469.
[43] D. D. Perrin, W. L. F. Armarego, D. R. Perrin, *Purification of Laboratory Chemicals*; Pergamon Press, Oxford, UK, **1980**.
[44] E. Rivarola, A. Silvestri, G. Alonzo, R. Barbieri, *Inorg. Chim. Acta* **1985**, *99*, 87.

[45] E. Kucharska, J. Hanuza, A. Waśkowska, Z. Talik, *Chem. Phys.* **2004**, *306*, 71–92.
[46] *SAINT*. Data Reduction and Correction Program. Version 8.34A. Bruker AXS Inc., Madison, Wisconsin, USA, **2014**.
[47] G. M. Sheldrick, *Acta Crystallogr., Sect. A* **2015**, *71*, 3–8.
[48] G. M. Sheldrick, *SHELXTL*, v. 6.14, Structure Determination Software Suite; Bruker AXS: Madison, WI, **2003**.
[49] G. M. Sheldrick, *Acta Crystallogr., Sect. C* **2015**, *71*, 3–8.
[50] G. M. Sheldrick, *SADABS*, v. 2.01, Bruker/Siemens Area Detector Absorption Correction Program; Bruker AXS, Madison, WI, **1998**.
[51] Y. Zhao, D. G. Truhlar, *Theor. Chem. Acc.* **2008**, *120*, 215–241.
[52] R. F. W. Bader, *Atoms in molecules: A quantum theory*, Oxford University Press, **1990**.
[53] T. Lu, F. Chen, *J. Comput. Chem.* **2012**, *33*, 580–592.

Received: July 4, 2018

P–N Adducts

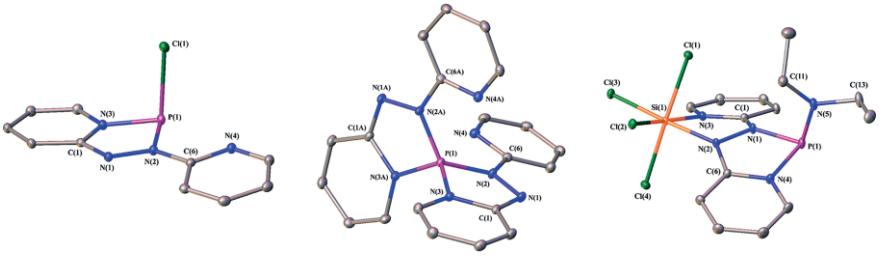

Like transition metals phosphorus may exist in different oxidation states in 2,2′-azobispyridine surrounding and change its valency by reactions of oxidative addition and oxidative elimination

DOI: 10.1002/ejic.201800831